2010

DC-DC Power Converter Design for Application in Welding Power Source for the Retail Market

Edward J. Oshaben
Cleveland State University

DC-DC POWER CONVERTER DESIGN FOR APPLICATION IN WELDING POWER SOURCE FOR THE RETAIL MARKET

EDWARD J. OSHABEN

Bachelor of Science in Electrical Engineering
Case Western Reserve University
May, 2005

submitted in partial fulfillment of requirements for the degree
MASTER OF SCIENCE IN ELECTRICAL ENGINEERING
at the
CLEVELAND STATE UNIVERSITY
December, 2010

This thesis has been approved

for the Department of ELECTRICAL ENGINEERING

and the College of Graduate Studies by

_____

Dr. Charles Alexander, Thesis Chairperson

_____

Department & Date

_____

Dr. Eugenio Villaseca, Thesis Advisor

_____

Department & Date

_____

Dr. Dan Simon

_____

Department & Date

_____

Dr. Ana Stankovic

_____

Department & Date

ACKNOWLEDGEMENTS

Thanks to Dr. Eugenio Villaseca of the Electrical Engineering department of the Cleveland State University, for his guidance in writing this thesis.

Thanks to Elliot Stava, Engineering Consultant to the Lincoln Electric Co, for his technical guidance with design approach.

Thanks to Theresa Spear, Design Engineer for the Lincoln Electric Co, for her technical guidance with design approach.

Thanks to the Lincoln Electric Company, for its support of this study.

DC-DC POWER CONVERTER DESIGN FOR APPLICATION IN WELDING POWER SOURCE FOR THE RETAIL MARKET

EDWARD J. OSHABEN

ABSTRACT

The purpose of this study is to design and analyze a DC-DC power converter for application in a welding power source that is cost-competitive with the more traditional, lower-tech welding power source topologies.

This thesis first presents a background study of recent design approaches to DC-DC power converters, as they relate to application in welding power converters. The background study also surveys recent design approaches to welding power source controls.

Evaluation of available options in DC-DC converter topologies and switching schemes for application in a welding power source is presented. Design methodology of a low-cost DC-DC converter for application in a welding power source is explained in detail. The design criteria are presented, and systematically solved for using a combination of electrical theory and computer-based modeling. The power converter design is modeled and verified through simulation.

An economic analysis of the design proves it to be economically feasible, but still not as inexpensive as traditional, lower-tech solutions currently in use in the

arc welding retail market. The most expensive component of the design is the power switching components, which have the potential for further cost reduction, and is recommended as future work.

TABLE OF CONTENTS

LIST OF TABLES

Table Page

LIST OF FIGURES

CHAPTER I

INTRODUCTION

Nearly all consumer electronics are powered by some form of DC-DC converters for either battery charging or electronics power supply regulation. Examples in battery-powered devices or in electronics include laptop computers, desktop computers, cell phones, and LED drivers. Another popular application of DC-DC converters in the consumer market is in power supplies for brushless DC motors. Examples of such applications include electric razors, CD/DVD disk drives, and battery-powered hand drills. An underlying theme of all of these applications is that they are relatively limited in power capability. The battery-powered applications are generally limited to less than 50 W of power due to the energy density limitations of existing battery technologies. The more powerful of retail consumer DC-DC converter applications reside in power supplies for personal computers, peaking out at around 1 kW of power.

The most prevalent avenue for delivery of higher power levels (1 kW – 5 kW) to the retail market is in constant-frequency AC motors. These motors are

designed to run off of 115 VAC or 230 VAC 50/60 Hz power, and are featured in table saws, corded electric drills, washing machines, dryers, pumps, and compressors, to name a few. It is the simplicity and cost-effectiveness of AC motors that make them commercially viable for higher power applications in the consumer market. All of these applications could conceptually be driven by DC motors with the help of DC-DC converters, but the economics of designing DC-DC converters proves to be unfavorable due to the large amount of silicon required to switch this much power. As a result, DC-DC converter technology at these power levels is only reserved for applications that require higher performance and functionality than what is needed for a retail consumer application, and therefore are less cost-sensitive since the industrial customer is willing to pay for the added functionality. Examples of these applications include DC motor drives for electric vehicles, converters for alternative energy generation and transmission, or industrial DC welding power sources.

The same analogy of AC motors vs DC motors can be made for choice of welding power source topology. The retail market remains highly cost-competitive, which drives the designer to favor reduced cost over added functionality. Additionally, the retail welding market does not have much need for advanced welding controls because they are not, for instance, making military grade welds that must adhere to strict strength and appearance standards. The analogy to AC motors in welder topology is the line-commutated transformer-rectifier (LCTR) power source. It is a relatively mature technology that is very

capable of delivering a large amount of DC welding power at a relatively low cost. The analogy to DC motors in welder topology is the inverter-driven DC-DC power converter (IDDD). It delivers more functionality at the same power levels as the LCTR, but at an added cost. Traditionally, when designing for a retail market, the welding power source designer chooses LCTR topology for its relatively low cost, simplicity of design, availability of materials, and reliability. Alternatively, if designing for a high-performance, high-power industrial market, the designer chooses the IDDD for its advanced welding waveform control, high efficiency, and ability to meet higher welding performance standards.

When one speaks of "welding performance", qualities that are considered include, but are not limited to, short-circuit response, weld spatter, arc stability, and weld bead appearance. All of these qualities are a product of the entire welding system, not just the power source. However, a more sophisticated control system, such as those used in the IDDD topology, will give the customer more control over the various welding waveform parameters, which in turn gives them more control of the weld quality in a given system.

In the retail welding market, the market needs are low cost, ease-of-use, good weld quality, portability, and a growing need for energy efficiency. The commonplace LCTR design topology currently meets the needs for low cost and ease-of-use relatively well. Weld quality is good; however the IDDD has the upper hand due to its ability to control the welding waveform. Portability and energy efficiency are not met very well by the LCTR topology, primarily due to the

weight and inherent energy losses of the welding transformer. IDDD already can serve the market needs of good weld quality, portability, and energy efficiency quite readily. If only the designer can improve upon the cost and ease of use of IDDD, then a welding power source product could be provided to meet all of the retail market needs better than either existing technology is currently capable.

LITERATURE REVIEW

The findings and results of [1] offered a 5 kW DC/DC converter solution for powering low-voltage hydrogen electrolysers from grid-connected photovoltaic energy sources. The challenges of their design include high voltage step-down ratio, galvanic isolation, wide input voltage range, and reliability. The design requirements differ from that of a retail welding power source in that the output load remains at a fixed operating point, and also that portability is not a requirement. These less stringent requirements result in the designers favoring low parts-count and simplicity over reduced size and cost. The solution consists of a hard-switched push-pull converter, using 1200V IGBT's, controlled by a simple PWM generator, and running at a switching frequency of 50 kHz. Switching noise is damped through the use of snubber circuits across both the primary switches and output diodes. Efficiency is in the neighborhood of 90%. The design likens to application in IDDD retail welding power sources in that it provides a high voltage step-down ratio and galvanic isolation, while supplying medium power at an acceptable efficiency.

A comparison study between analog and digital controls for a PWM generator in a Buck converter application is presented in [2]. Given a known model of the plant, the authors derive 3 different PWM control methodologies: (1) tuned analog PID, (2) explicitly solved digital control, (3) sliding mode controller design. The controllers are each simulated in Matlab/Simulink, and regulation is tested in simulation using instantaneous load step change at the output of the Buck converter. Simulation results proved that both the tuned analog PID and the sliding mode controller significantly outperform digital control (sliding mode control is also implemented in analog). Both types of analog control yield faster response time and less deviation from the reference signal than with digital control. The disadvantage of digital control in this case can be explained by the processing delays in the A-D converter, which is limited by its quantization level. A change in the error signal will not drive a change in the digital controller input signal until a quantization level of the ADC is reached. Meanwhile, the error signal in either analog design is continuously fed back to the controller, and thus can drive infinitesimal change to the control signal. Another disadvantage of the digital controller is that there is a delay of one switching period in order for the control signal to update, whereas the analog controllers are capable of immediate adjustment of the control signal. Comparison is also made between the tuned analog PID control and the sliding mode analog control. Simulation results are extremely similar for both; however the sliding mode control does prove to be faster and more regulated, with its only drawbacks being slightly longer settling

time and its inability to maintain constant frequency switching during load transients. It is admitted that digital control offers greater flexibility in application, however that always comes at some finite amount of cost in closed-loop response time.

These same arguments can be made for comparison of welding control methodologies. For industrial welding solutions, demanding finely tuned and optimized welding waveforms in order to minimize weld time without sacrificing weld integrity, digital control certainly has the upper hand at configurability. For this reason, an industrial customer would be willing to pay for the added functionality and inherent cost of high-performance digital processing. On the other hand, less demanding welding applications such as those found in the retail market, where an average constant steady-state arc voltage or current is the predominant requirement, do not necessitate the configurability offered by digital controllers. In this case, analog control can be utilized to the extent of its application, to offer fast response to load and source variations with minimal design complexity.

Direct application of novel DC-DC converter switching schemes and topologies in welding power sources have been published as well. A phase-shifted control scheme is proposed for a half-bridge topology in [3]; specifically for application in high current/ low voltage output power requirements found in arc welders. Advantages of the proposed converter include lower voltage stresses on the switching components, power conversion efficiency ranging from 85% to

90% (depending on loading level), zero-voltage switching at turn-off of all switches, and zero-voltage/ zero-current switching at turn-on of all switches. Since the converter uses a half-bridge topology, the high-frequency link transformer only sees half the input bus voltage during a given energy transfer stage. As opposed to a full-bridge topology, the half-bridge will in turn drive the need for lower turns-ratio in order to achieve the same amount of output open-circuit voltage, which is needed for proper arc-starting in welding applications. As a consequence of lowered turns-ratio, primary currents will be higher for a given output welding current, which will necessitate more silicon in switching devices and more conductor weight in primary windings in order to maintain given conduction losses in the primary circuit. The proposed topology shows definite promise for applications having high supply line voltages (300 VAC or greater). However, its feasibility for use with residential input voltage (110-240 VAC, 1-Φ) has yet to be tested, and is at a natural disadvantage to the full-bridge for these reasons.

The proposed converter of [3] was an improvement over a previously proposed converter by the same authors in [4]. The converter proposed in [4] can be realized in either half-bridge or full-bridge topologies, and utilizes active-edge resonant cells (AERC) to accomplish soft switching. Duty cycle control is implemented with symmetrical PWM as opposed to phase-shifted PWM control. The proposed converter has potential application in high performance arc welders; however the added complexity of AERC as well as an additional auxiliary active inductor cell

for soft switching under light loading conditions does not make it a good candidate for low-cost retail solutions. The paper does touch on the PID inner and outer loop control concept, which may be used to draw comparison to the control scheme chosen in this research.

Simulation study and prototype verification of a double-closed-loop controller for an arc welder is discussed in [5]. Transfer functions for the voltage and current controllers are presented for controlling a simple half bridge converter. Dynamic load response is evaluated and optimized under the double-loop controller. Results of the study prove a high feasibility for a simple low-cost converter for arc welding, the controls of which can be completely implemented with analog circuits. However, both the simulation and experimental results are only presented for a single load operating point, so the flexibility of the proposed control scheme has yet to be proven.

The power converter discussed in [6] addresses some valid concerns with designing for high-frequency operation. With the advancement of the DSP in recent years, faster response times can be attained by increasing the switching frequency. One problem posed by higher switching frequencies is the decreasing ability of the electrolytic input filter capacitor(s) to conduct bridge commutation currents. This is attributed to the inductive behavior of electrolytic capacitors above 100 kHz. The proposed converter of [6] utilizes commutation capacitor banks consisting of multiple paralleled capacitors to maximize commutation capability. Other features of the proposed converter include lowered inrush

current, which eliminates the need for a soft-start circuit. The practice of including bridge commutation capacitor banks to supplement the main filter capacitors will also be implemented in the proposed converter resulting from this thesis project.

The converter and control scheme discussed in [7] is more focused on the control methodology for double-pulsed gas-metal-arc-welding (DP GMAW). DP GMAW is a pulsed waveform output which facilitates more control of weld bead appearance. The proposed converter of [7] exploits the flexibility of the DSP, which makes it an ideal control solution for a more complex arc waveform, such as DP GMAW. The DSP is also used to generate the PWM signal for a zero-voltage-switched phase-shifted full-bridge (ZVS PSFB) as the choice for converter topology and switching scheme. Valid points are made for advantage of using digital controls over analog for PWM generation, such as flexibility, no temperature shift, and higher precision. One argument that the authors fail to address, however, is the closed-loop delays incurred with digital PWM generation. Since the PWM is integrated into the function block of the DSP, delays are incurred with A/D conversion and PWM computations. If the function of PWM generation were chosen to be an analog inner control loop instead, near instantaneous response times can be achieved for an instantaneous change in load, such as that seen in the welding arc. The key advantage of including the DSP as part of the inner control loop, as the authors point out, is its flexibility in application. The various tunable parameters involved with generating the PWM can all be modified through software as opposed to changing analog components

in the error amplifier or PWM circuit. Details are also discussed on the DP GMAW control method, as well as synergic control of wire feed speed. Synergic control is one which actively controls the wire feed speed in proportion to the welding current. The proposed converter of [7] is sized for 20 kW of output power, which is certainly outside of the scope of retail welding applications, but does appear to be a very feasible solution for higher performance industrial applications.

Analysis of an FPGA-based digitally controlled welding power source is presented in [8]. Vast improvements over a microprocessor-based solution is claimed by attaining a 65 ns timescale using new FPGA architectures versus a 300 µs timescale using a 12 MHz microprocessor. The fastest welding process times are known to be in the range of 100 ns [9], so the FPGA-based control is claimed to have better welding performance due to its smaller timescale. All else equal, when comparing the proposed FPGA control against the original partly analog control used in an existing 500A 50V arc welding machine, the reference tracking step response of the FPGA control is experimentally verified to have less overshoot and similar response time as the partly analog control. The completely digital control is achieved while only using 27% of the FPGA's resources. The only experimental data presented or mentioned of is the inner loop step response of the controller, which would be the simplest and fastest response time that could possibly be analyzed. Nothing is mentioned of the comparative performance of the outer loop response time, which would include additional processing time to

recalculate the reference signal level under dynamic loading conditions, which are typical of the welding arc load. This potentially could be an advantage for the partly analog control with regards to response times since it uses a different method of calculating and driving the reference signal. Cost-effectiveness is not discussed either; however board space may likely be minimized by consolidating the various control loop functions to a single FPGA. Another obvious advantage of the FPGA-based design is its flexibility and scalability to various processes and applications.

PROBLEM STATEMENT

The problem with designing an IDDD for the retail market is its cost compared to the LCTR. Primary cost components of IDDD welding topology are the controls, the power switching devices and/or associated heat sinks, and the power conversion transformer. The converter must provide isolation from the mains supply; therefore the less expensive options for DC-DC converter topologies, such as buck converters, may not be considered for this application. The goal of this study is to design and analyze an IDDD welding converter, which is cost-competitive with LCTR, by simplifying the controls electronics, utilizing the newest technologies in power electronics for the inverter engine, and reducing the size of the power conversion transformer.

Chapter 2 introduces the control scheme, and presents its advantages over traditional IDDD control schemes. Chapter 3 discusses options for the DC-DC converter topology and their associated tradeoffs. Chapter 4 discusses options for

the inverter engine, including choice of semiconductor technology and switching scheme, and their associated tradeoffs. Chapter 5 presents a working model for simulation and product design. Chapter 6 presents an economic analysis of the proposed design. Chapter 7 concludes the work by summarizing the results, discussing its contribution to the state of the art, and proposing future work.

CHAPTER II

CONTROL SCHEME

The choice of control scheme is influenced by multiple factors. Since the purpose of the design is to achieve inverter-driven welding control at a cost that is competitive with LCTR technology, the choice of control scheme is heavily influenced by this same criteria. Microprocessor-based control lends itself to flexibility in multiple product platforms. Due to its flexibility, a single controller design could be extended across a wide range of machines marketed for various welding processes and power levels, differing only by the controller software. As the controller gets extended to more applications, its production volume increases, and thus the quantities of the electronic components required to manufacture the controller also increase. If those quantities are high enough, cost breaks can be achieved by buying larger lot sizes, thus reducing the cost of the controller. On the other hand, microprocessors are relatively expensive even at high volumes, and reduced material costs must be partially offset by increased software development

costs. Additionally, closed-loop response times are relatively slow due to signal processing delays incurred within the microprocessor.

Analog control resides at the opposite extreme with regards to the economics of design implementation. An analog controller is tuned for a specific process, which prevents it from being extended across platforms. Electronics components are relatively low cost, however the complexity of the hardware increases exponentially with added functionality. In order to attain the basic functionality required for welding control while driving an inverter engine, board space rapidly grows to accommodate the various functions. Power density is lowered and the overall cost of the PCB blank material itself grows. Closed-loop response time is relatively fast given proper tuning.

Both extremes present advantages for their respective niche. Digital control offers highly-integrated functionality and flexibility. Analog control offers low component costs and faster signal propagation. An intelligently designed controller should use both control schemes in hybrid to perform explicitly what each is better suited to do. A block diagram of the proposed hybrid control scheme is shown in Figure 1.

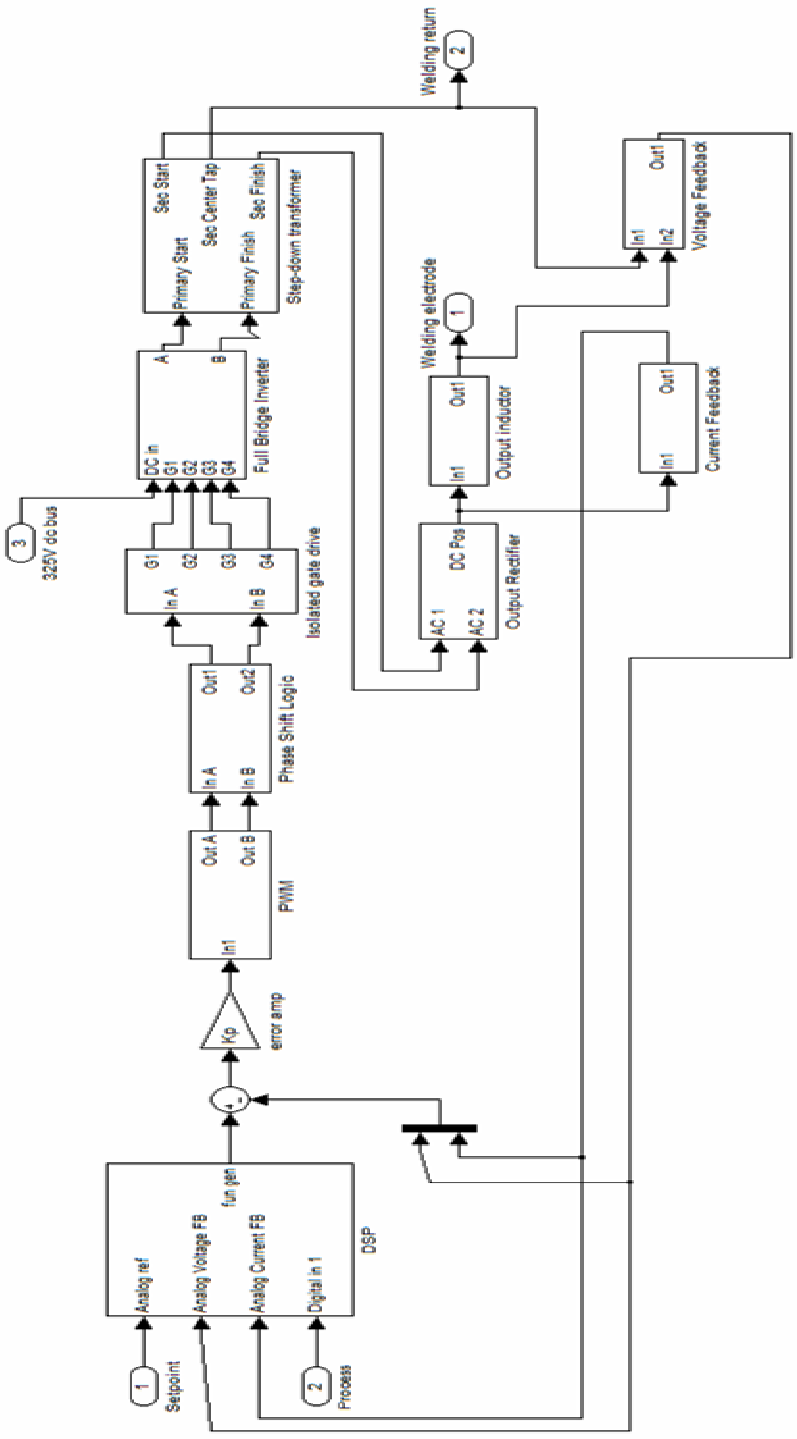

Figure 1
Power Converter Block Diagram

The following is an overview of the power converter blocks.

The DSP block consists of a single digital signal processor IC. Its primary purpose is to control the function generator which represents the current or voltage reference signal (depending on which mode of operation the welding state logic programmed within the DSP is dictating). It accepts the user inputs from the control panel of the welder, processes those inputs to determine its initial state, creates a reference tracking signal based on its current state, and processes the current and/or voltage feedback signals to determine what its next state should be. The cycle repeats itself based on its new state. As the state of the welder control changes, so does the value of the reference tracking signal, resulting in a time-domain function generator output.

The error amp is a traditional proportional gain amplifier which amplifies the error between the reference tracking signal and the current or voltage feedback signal, based on its theory of operation to force the difference between its two inputs towards zero. The DSP dictates which mode of control (current-controlled or voltage-controlled) is being used, and thereby selects which feedback signal gets fed into the error amplifier.

The purpose of the PWM block is to indirectly control the duty cycle of the primary switches within the full bridge inverter. “Out A” and “Out B” are digital signals that represent the respective ON-times of the two halves of a *traditional* full bridge converter. This application utilizes a *phase-shifted* full bridge however, and hence the PWM outputs do not directly control the full bridge gate timing.

Instead, they drive the phase shift logic which in turn determines the gate-timing for the full bridge. What does hold true, however, is that larger duty cycles driven by the PWM block still equate to larger duty cycles of the full bridge. The average pulse widths of the two outputs are typically equal in order for the transformer core to not saturate.

The phase-shift logic converts the pulse trains from the two PWM outputs into phase-shifted gate drive signals. The primary purpose of using phase-shifted gate drives is to reduce electrical switching noise and to accomplish zero-voltage switching in the full bridge inverter. The functionality of phase-shifted gate drives will be explained further in Chapter 4.

The isolated gate drive block converts the two gate drive signals from the phase-shift logic block into four inter-dependent gate drive signals. The outputs of the block are galvanically isolated from the inputs through the use of pulse transformers. Isolation of the full bridge inverter (which is common with the input mains) from the controls (which are common with welder output) is a regulatory requirement for the prevention of electrical shock to the welding operator. The isolated gate drive block also provides a power buffer which is needed to quickly supply and displace charge out of the gates of the full bridge inverter in order to accomplish fast switching times and saturated operation of the switches within the full bridge inverter.

The function of the full bridge inverter is to *efficiently* invert the mains dc bus supply, typically 325 Vdc, into a single-phase, 100 kHz, 3-level square wave. Its 3

levels of output are equal to positive dc bus, zero, and negative dc bus. It is the high-frequency characteristic of the full bridge inverter which reduces the required size of the magnetic components in the remainder of the power converter; namely the step-down transformer and the output inductor.

The step-down transformer has four primary functions: galvanic isolation, voltage/current transformation, free-wheeling energy storage, and frequency doubling.

Galvanic isolation is required to isolate the welding circuit from the input mains. For the same reason as for the use of pulse transformers in the isolated gate drive block, galvanic isolation of the welder output from the input mains is a regulatory requirement and improves safety to the welding operator.

Voltage/current transformation is required to step the input dc bus voltage (325Vdc nominal) down to typical arc welding voltages (<70 Vdc) via the transformer turns ratio. The goal for output current capability is 400 Amps into a short-circuit. Current transformation performed by the step-down transformer reduces the current amplitude through the inverter switches, which serves to keep the devices operating within their device ratings.

Free-wheeling energy storage is needed to accomplish zero-voltage switching in a phase-shifted full bridge inverter. The leakage inductance of the transformer is typically viewed as a nuisance parasitic element, because it adds unwanted impedance to the supply circuit. However, with the use of a phase-shifted full bridge inverter, some leakage inductance is needed to aid in commutating the

bridge. The transformer leakage inductance stores energy during the energy transfer stage, and releases energy during the free-wheeling stage, and will be discussed in more detail in Chapter 4.

Frequency doubling is achieved by the center-tapped secondary winding configuration of the transformer. This doubles the ripple frequency of the dc welding current, which reduces the required size of the output inductor.

Continuing with the descriptions of the blocks of the power converter, the output rectifier simply converts the AC voltage waveform from the step-down transformer to an unfiltered DC voltage waveform. DC voltage and current is required for most welding processes used in the retail market.

The output inductor helps to smooth the welding current ripple at the lower end of welding current range. The welding arc is more stable when there is less ripple in the current. The current ripple is only noticeable at lower current outputs, and therefore the output inductor is designed to saturate at approximately 100 Amps so that it does not impede current flow when larger welding current is needed.

The current feedback block creates an analog voltage signal which is proportional in magnitude to the welding current. This is needed to close the loop on both inner and outer control loops.

The voltage feedback block creates an analog voltage signal which is proportional in magnitude to the welding arc voltage, which is also needed to complete both the inner and outer control loops.

Analog controls are primarily used to implement the inner loop, while a DSP is used to control the outer loop. The goal of the inner loop is simple: to minimize the error between the reference signal from the DSP and the output feedback. In a microprocessor-based control scheme, the functions of error amplifier, PWM, and phase shift logic may all be integrated into the microprocessor. The purpose of peeling those functions out of the digital control block in the proposed control scheme is to minimize the computational requirements of the DSP and also speed up the response time of the inner control loop. By minimizing the computational requirements of the DSP, a smaller, less expensive one may be chosen for the design, while still utilizing its functionality where it is needed most: the function generator. The goal of the outer control loop is to control the welding process function generator. It is dynamically commanding how much current or voltage to make at the output based on its programmed knowledge of the desired welding process and the feedback signals. Note that the controller explained thus far is strictly for the output power regulation of the welder. Additional welding controls are required for the wire feeder motor, however that is outside the scope of this research.

CHAPTER III

CONVERTER TOPOLOGY

There are five main categories of *isolated* dc-dc converter topologies [10]. They are 1) Flyback, 2) Forward, 3) Half-Bridge 4) Full-Bridge 5) Push-Pull. The output rating of the welder being designed in this study is earmarked for 150 Amps at 23.5 Volts, as determined by market needs and other competitive products. That means the power converter must be capable of supplying 3.5 kW of power for extended periods of time without thermal or electrical stress to the converter. Of the five converter categories named above, only two of them are typically recommended for off-line applications at this power level: the Full-Bridge and the Push-Pull (Figures 2 and 3). Flyback converters can not be used because they are limited in output current capability. Half-Bridges are difficult to control using current-mode control, and require additional circuitry to prevent saturation of the transformer. Forward converters are limited in power level because they can only drive the transformer in one direction, and must remain under 50% PWM conduction to allow for the transformer to reset its flux density.

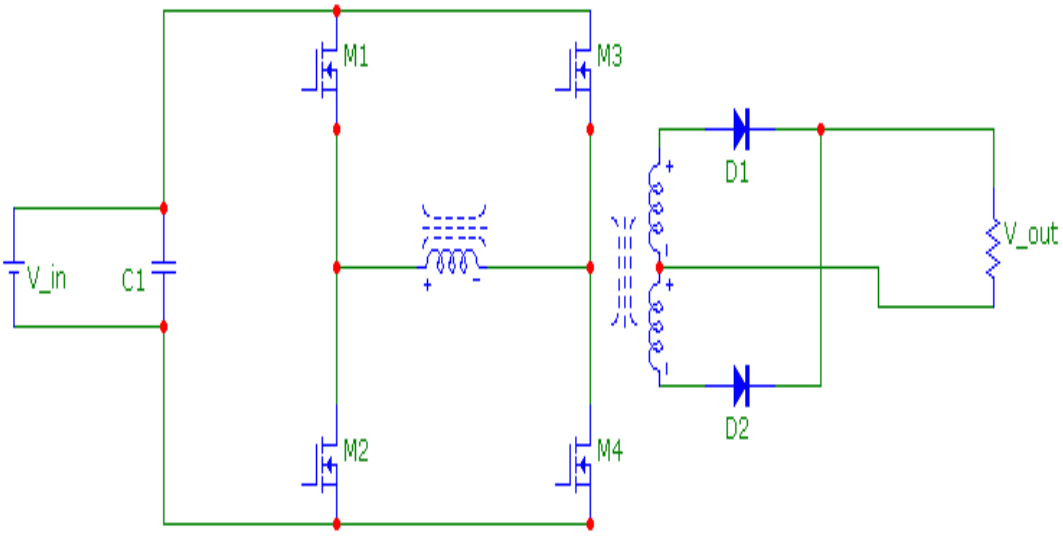

Figure 2
Full-Bridge Topology

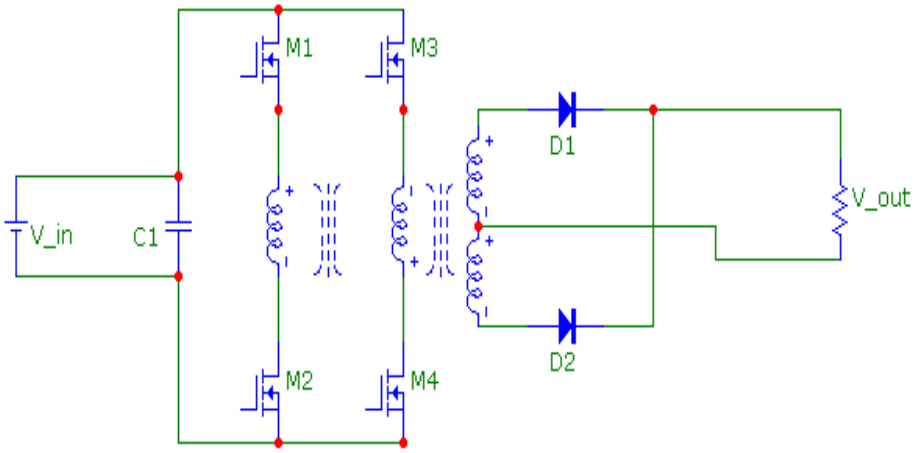

Figure 3
Push-Pull Topology

The input voltage level in conjunction with the choice of converter topology will determine the maximum amount of voltage seen across the switching devices. If a Push-pull converter were to be used, the natural choice would be a "two-sided" Push-Pull, which limits the voltage stress across any one switching device to the input bus voltage. Using "single-sided" topology would require switching devices with a minimum of twice the voltage rating of those in the "two-sided", which results in switching devices that have inherently higher on-state resistance due to their higher voltage rating, and hence more losses. The Push-Pull also requires a more complicated transformer design than with the Full-Bridge, as it utilizes two independent primary windings. Each winding drives the transformer in a single direction, which requires that twice the number of total primary turns are needed in comparison to the Full-Bridge. The more complicated transformer design necessitated by the Push-Pull will be a significant cost-adder to the overall design.

If a Full-Bridge topology is pursued, all of the benefits of a two-sided Push-Pull converter are still achieved, with one drawback being the potential for cross-conduction failure of the bridge in the case of gate misfire. Since a smaller transformer is realized with the Full-Bridge, and all other material requirements are equal to that of the Push-Pull, the more economical choice is the Full-Bridge. Another advantage of using a Full-Bridge topology is the opportunity for phase-shifted switching. The primary advantage of using phase-shifted switching is lower switching noise, lower switching losses, and no need for snubber circuits

across the switches. Phase-shifted switching will be discussed further in Chapter 4. Lowered switching noise in lieu of phase-shifted switching also eases the initial concern of cross-conduction failure due to gate misfire. Since high frequency switching noise is significantly lowered, there is little potential for noise coupling to the gates of the switches and causing false firing. Attention will still need to be given to the PWM gate drive control to ensure that no circumstance can result in accidental cross-conduction.

For the above-stated advantages over the Push-Pull topology, a Full-Bridge topology will be used in the proposed welder.

CHAPTER IV

SWITCHING SCHEME

In order to improve efficiencies and potentially reduce the cost of heat sinking and/or silicon used, phase-shifted switching scheme is utilized. As stated in the previous chapter, the advantages of phase-shifted switching include reduced switching noise, reduced switching losses, and no need for snubbers across the switching devices. Since the cost of the main transformer is expected to be a significant contribution to the overall cost of the welder, effort is placed to minimize the transformer's overall size. Transformer size can be reduced by raising the switching frequency of the welder, and thus attaining the same peak flux density for a smaller amount of cross-sectional area of the ferrite core. One general limitation of raising the switching frequency is the resultant increase in switching losses, since the switching losses are proportional to the switching frequency. By utilizing phase-shifted switching, we achieve zero-voltage-switching (ZVS) upon device turn-on, and thus cut the switching losses nearly in half.

ZVS may also be achieved using a resonant converter instead of phase-shifted switching, however since phase-shifting is implemented in the low-voltage gate drive circuit using inexpensive digital logic as opposed to large bulky analog components in the power section of the resonant converter, the obvious choice for ZVS is with the phase-shifted switching scheme.

An overview of phase-shifted full-bridge switching operation can be found in [11]. In brief, the primary winding of the full bridge transformer is always tied to a reference point on the dc input bus, and is never left floating, even when the converter is not transferring power to the load. This provides a path for inductive current to gracefully commutate from one quadrant of the bridge to another without voltage transients being induced in the switching circuit.

ZVS is achieved through the parasitic output capacitance of a given switching device resonating with the leakage inductance of the transformer immediately following switch turn-off. This charging of the device output capacitance creates a ZVS condition for the opposing common-leg switching device (i.e. M1 and M2 are common-leg devices shown in Figure 2).

In a hard-switched converter, snubbers are needed in order to absorb and dissipate voltage and current transients on the switching devices. Since these transients are reduced by orders of magnitude in a phase-shifted converter, snubbers are not needed, further reducing cost and improving efficiency.

One additional benefit of lowered switching noise is reduced EMI, and hence reduced need for EMI shielding. This can have a significant impact on total PCB

cost as less board material is needed to space apart circuit layers which may otherwise interfere with each other. Ideally, a hard-switched converter board that is distributed between 4 PCB layers, for example, may be reduced to 1 or 2 layers once all of the EMI associated with hard switching is eliminated using a phase-shifted converter. Such improvements can lower total PCB cost by 25-50%.

CHAPTER V

MODEL

A working model was developed to aid in designing a prototype. Electronic component parameter settings and design techniques were chosen through the use of this model. Worst-case scenarios, such as low input voltage, high input voltage, maximum loading, minimum loading, short-circuit loading, etc., were simulated to determine what the correct choice for various circuit components should be in order to meet the design constraints, which are as follows.

EXPLANATION OF DESIGN CONSTRAINTS

1) Must be capable of supplying 180 ADC into a 23 VDC welding load (arc); with a nominal full-wave-rectified and filtered input supply of 230 VAC, single-phase. The 120 Hz ripple of the output current shall not exceed +/- 9 Amps (+/- 5% of average value) into a static resistive load. This 120 Hz ripple is attributed to the operating frequency (twice the AC mains frequency) of the input rectifier.

2) Must be able to supply 400 ADC into a 1 VDC welding load (arc shorted); with a full-wave-rectified and filtered input supply of 207 VAC (230V - 10%), single-phase.

3) Must be able to supply a minimum of 35 VDC into an open-circuit load (arc starting); with a full-wave-rectified and filtered input supply of 207 VAC (230V – 10%), single-phase.

4) Must be able to supply 150 ADC into a 23.5 VDC welding load (arc) at a 30% duty cycle using ten-minute periods without the steady-state temperatures of the applicable insulations exceeding their respective temperature ratings. Applicable insulations include those used on the step-down transformer and in the isolated gate drive, as well as those used in the printed circuit board material.

5) The peak-to-peak 200 kHz ripple in the output current must not exceed 10% of its average value. The 200 kHz ripple is attributed to the operating frequency (twice the inverter frequency) of the output rectifier. This criterion will be most difficult to meet when at minimum load state. The minimum output rating of the power source is 30 ADC into a 15.5 VDC welding load (arc). Therefore, the maximum allowable peak-to-peak output current ripple is 3 Amps.

6) Must not exceed the thermal or electrical ratings of any of the electrical components under any allowable operating condition.

7) Favor low cost over high performance.

The converter topology and switching scheme has already been defined as a phase-shifted full-bridge. The design parameters which must be set in order to

meet the design criteria include input bus capacitance, choice of full-bridge switching devices, number of switching devices, transformer turns ratio, number of primary turns, transformer leakage inductance, transformer core area, choice of output rectifier devices, number of output rectifier devices, output inductance, choice of gate driver IC's, choice of PWM controller IC, choice of phase-shift logic implementation, choice of gate-drive transformers, control power supply specifications, cooling system design, choice of DSP, error amplifier design, and current and voltage feedback circuit design.

Some of these design parameters are assumed as given because this design is an extension of a pre-existing design. The given design choices are primarily associated with the welding controls. They are the DSP, error amplifier design, and feedback circuit design. The remaining design parameters are determined in consideration of the design criteria.

TRANSFORMER CORE DESIGN

The design process will now be discussed. As stated earlier, an important design criteria is low cost. Transformer size and material cost can be lowered by choosing a high operating frequency due to its effect of lowering the flux density of the transformer, and enabling the use of smaller ferrite cross-sectional area. Given that my other design experience with inverter-driven welders is with operating frequencies in the range of 20 kHz – 30 kHz, an operating frequency of 100 kHz was chosen as a starting point for the design. This would effectively

reduce the size and material cost of the magnetics by 80% as compared to familiar designs running at 20 kHz.

Transformer cross-sectional area was chosen to prevent saturation under the worst-case line voltage conditions. The ferrite material type chosen is recommended for 100 kHz operation and begins to saturate at about 300 mT at 100 degrees Celsius. For a constantly applied voltage, the equation for flux density excursion is

$$\Delta B = \frac{V \Delta t}{NA} \qquad (1)$$

Assuming a 10% high input line voltage of 253 VAC (357 VDC after full-wave rectification and filtering), 100% on-time in the bridge, 5 primary turns, and balanced operation of the ferrite core, the minimum cross-sectional area to prevent transformer saturation is 6 sq cm. The choice of 5 primary turns will be explained later in this chapter. Using 6 sq cm of ferrite cross-section, the flux density will swing from -300 mT to +300 mT as 357 VDC gets applied for 5 μs in each polarity. During transient conditions, the transformer may become imbalanced without the use of controls to detect transformer saturation. Pulse-by-pulse current limiting is a common way to prevent such transformer saturation, and will be utilized in this design. However, those controls should only come into play during transient conditions. During steady-state operation, we want the transformer to operate within some comfortable margins of safety from saturation. Therefore,

allow for a 20% safety margin, and the design choice for ferrite cross-sectional area is 7.2 sq cm.

FIRST DESIGN CONSTRAINT

Choice of input storage capacitance is primarily determined by the maximum load requirement and 120 Hz maximum output ripple limit. From the first design criteria, the welder must be able to supply 180 A at 23 V, and have no more than ±5% ripple contributed by the 120 Hz AC voltage component across the input storage capacitor. Ideally, the full bridge should be able to regulate the maximum output without reaching 100% of the maximum conduction time, as indicated by the error signal reaching its available limit. When the bridge is within regulation, the error amplifier can compensate for most of the input storage capacitor supply voltage ripple. As the input capacitor discharges, the error amplifier can gradually increase the conduction time in order to maintain a constant output voltage for a falling supply voltage. If the bridge reaches full conduction time while trying to maintain a constant output, then the bridge will no longer be in true regulation, and the output voltage will be determined by the passive parasitic elements of all of the power stage components. This is not desirable because it is difficult to control these parasitic elements in a realistic manufacturing environment. The result could be the inability to meet the output requirements if any of the parasitic elements drift too far from their known operating points.

The choice of input storage capacitance will determine how far the DC supply voltage falls before getting re-charged by the mains supply. The capacitance

should be just large enough so that the error amplifier does not reach its available limit in order to make the maximum output. Through simulation, the converter can utilize a DC supply voltage down to 265 VDC while making its maximum output before it falls out of regulation. In order to allow for some safety margin, the input storage capacitance is chosen so that the capacitor voltage falls to no lower than 278 V, which is 5% above the 265V deregulation point. The resultant capacitance value is 2200 μF. Using this capacitance, the 120 Hz output current ripple is ±2.7% of the average value of the output current, which is within the design criteria of ±5%.

The model was built and simulated in Microcap 9 software environment. The output current and output voltage waveforms at a 180 A, 23 V load, along with the input storage capacitor voltage waveform are shown in Figure 4.

SECOND DESIGN CONSTRAINT

According to the second design criteria, the converter must be able to supply 400 ADC into a 1 VDC welding load (arc shorted); with a full-wave-rectified and filtered input supply of 207 VAC (230V - 10%), single-phase. This is not a concern with regards to the output power capability of the converter, since this is only 400 W of power in comparison to the 4140 W power capability proven by meeting the first design constraint. The challenge in supplying 400 Amps is to keep the current density through the primary switches within a safe operating area. Increasing the turns ratio of the transformer will proportionally lower the primary current, while yielding the adverse effect of lowering the available output voltage

to supply to the load. For this reason, the transformer turns ratio should be chosen to be as high as possible while still supplying enough output voltage to meet the maximum output requirements.

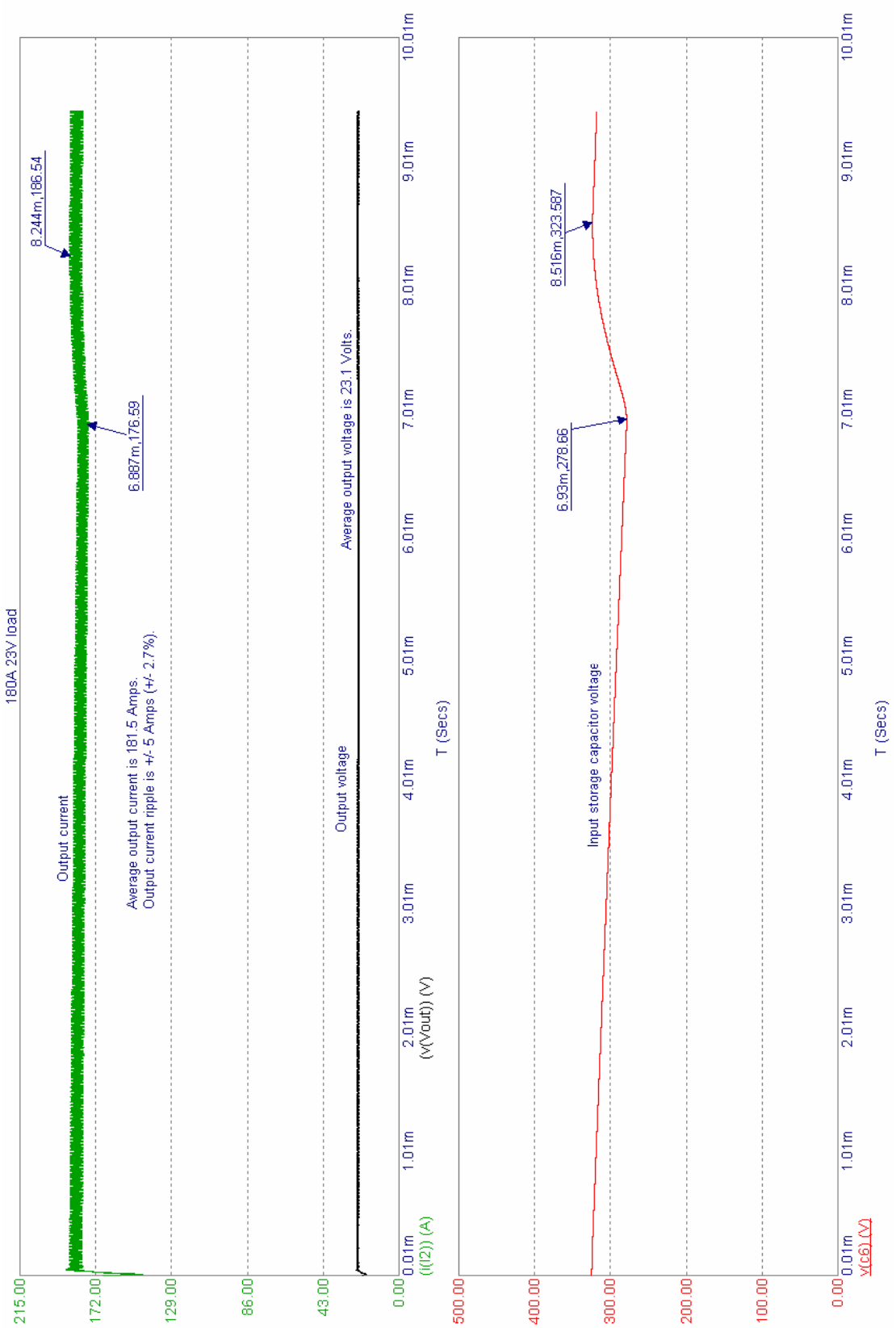

Figure 4
180A 23V Load

Through investigation by simulation, the ideal turns ratio is 5:1. With a turns ratio of 5:1, the converter can regulate maximum output while still tolerating the ripple in the input capacitor voltage. A turns ratio of 5:1 implies that a magnitude of one-fifth of the output current will be flowing through the primary circuit during the power transfer stage of the converter. For a 400 ADC output, there will be a peak current of 80 A flowing through the primary switches.

Plots of the output voltage and current, along with the primary winding voltage is shown in the top half of Figure 5. From the simulation results, it is verified that the second design criteria is met. Plots of the primary winding current and the current through one of the primary switches are shown in the bottom half of Figure 5. From these simulation results, it is verified that the peak current flowing through the primary switches is 80 A.

Since a 400 ADC, 1 VDC load is a typical operating point for a welding power source, the primary switches must be capable of conducting the 80 A peak current flow at the resultant PWM duty cycle without thermal stress to the silicon die. The switch chosen for this application is Fairchild part FCH76N60N (600V N-channel MOSFET). According to the simulation results shown in the bottom half of Figure 5 and performing some simple calculus, the equivalent *square-wave* pulse duration through the switch with a magnitude of 80 A is 2.1 μs. Given a switching period of 10 μs, the equivalent square-wave pulse duty cycle is 21%. Using the Transient Thermal Response Curve of [12], the junction-case thermal impedance of the MOSFET during this loading condition is .045˚C/W.

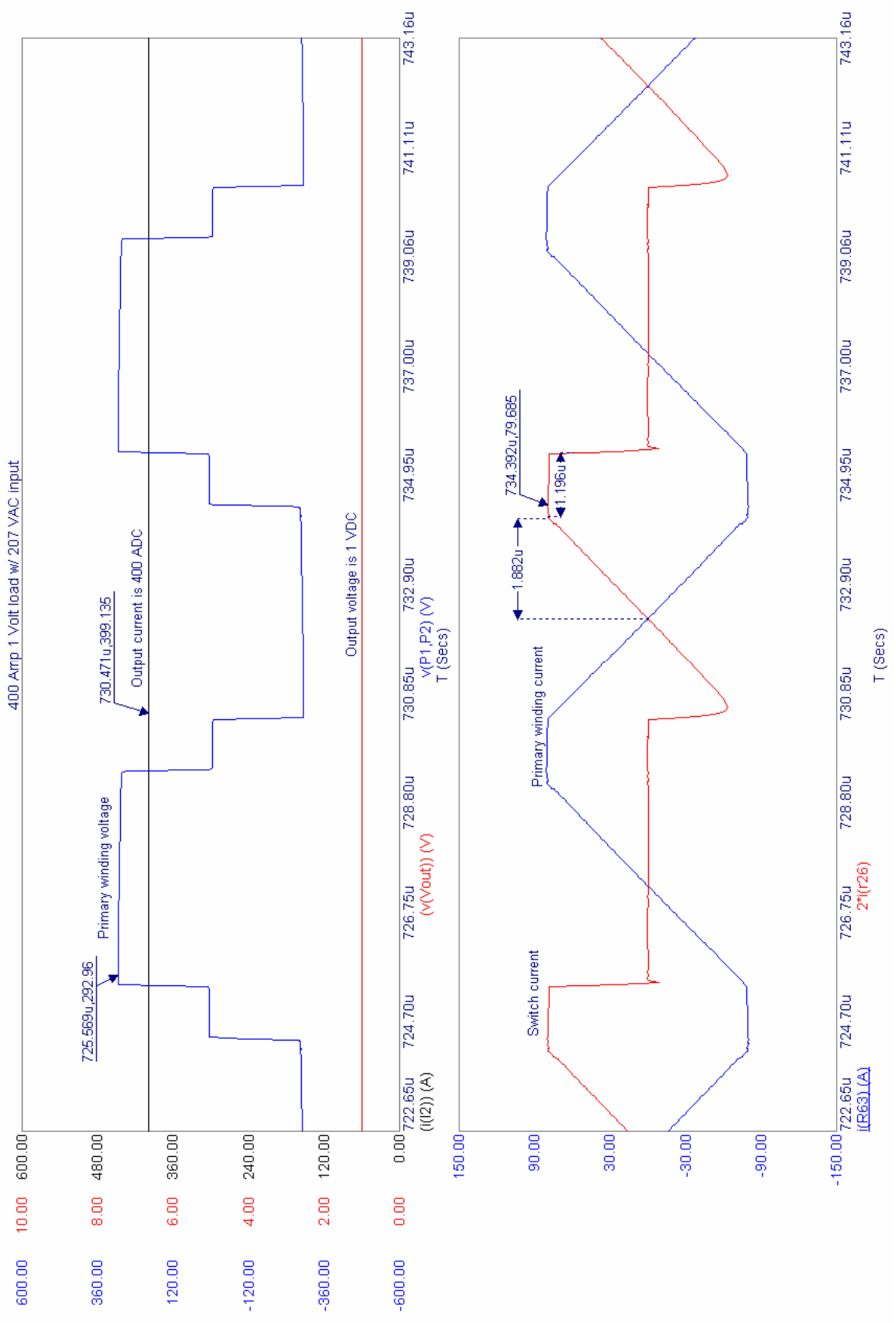

Figure 5
400A 1V Load

The maximum junction-case temperature rise can be calculated from the equation

$$T_{JM} - T_C = P_{DM} Z_{\theta JC} \qquad (2)$$

where P_{DM} is the instantaneous power dissipation of the MOSFET during the pulse, and $Z_{\theta JC}$ is the junction-case transient thermal impedance. The instantaneous power dissipation can be calculated from the equation

$$P_{DM} = i_D^2 \; R_{DS(ON)}(T) \qquad (3)$$

Assuming the on-state resistance is at its maximum during the pulse is a conservative approach to predicting the power dissipation. Therefore, the value for $R_{DS(ON)}$ is assumed to be at the maximum junction temperature of 150˚C, which is 93 mΩ [12]. Plugging this value into (3), the instantaneous power dissipation is 595.2 W at a maximum junction temperature of 150˚C. Plugging the result of (3) into (2), the maximum junction-case temperature rise during the 400 A, 1 V loading condition is 26.7˚C. This implies that in order to keep the junction below its critical temperature, the MOSFET case must be kept at least 26.7˚C below that critical temperature under any condition preceding the 400 A, 1 V loading condition. According to the datasheet, the maximum rated junction temperature is 150˚C. In order to allow for some safety margin, the design target is to keep the junction temperature below 120˚C, and hence the case temperature below 93.3˚C. A conservative approach is to assume worst-case ambient air temperature to be

40˚C, so this provides for a maximum case-ambient temperature rise of 53.3˚C. Therefore, the heatsink must be designed to meet or exceed this constraint.

THIRD DESIGN CONSTRAINT

According to the third design constraint, the converter must be able to supply 35 VDC into an open circuit (no load) with an input voltage of 207 VAC. After full-wave rectification and filtering of the input supply, the storage capacitor voltage is 292 VDC. Thanks to our design consideration of minimizing the turns ratio earlier, it will be easy to meet this design constraint. If the bridge is operating at 100% conduction time, the output voltage will be 58.5 V at its peak. Without the use of any output storage capacitor, the no-load output voltage waveform takes the shape of a 200 kHz full-wave-rectified AC signal, which drops down to zero and quickly returns back to its peak positive voltage. Given this lack of output filtering, the average output voltage determined from simulation is 44 VDC when the bridge is at it maximum allowable conduction time. This exceeds our requirement of 35 VDC, including an additional safety margin of 25%. The plot of the maximum no-load output voltage with an input supply voltage of 207 VAC is shown in the upper half of Figure 6. The bottom half of Figure 6 shows plots of the primary winding voltage (red) and primary winding current (blue) under these same conditions. The primary winding current is consumed solely due to magnetization, otherwise known as excitation, of the ferrite core.

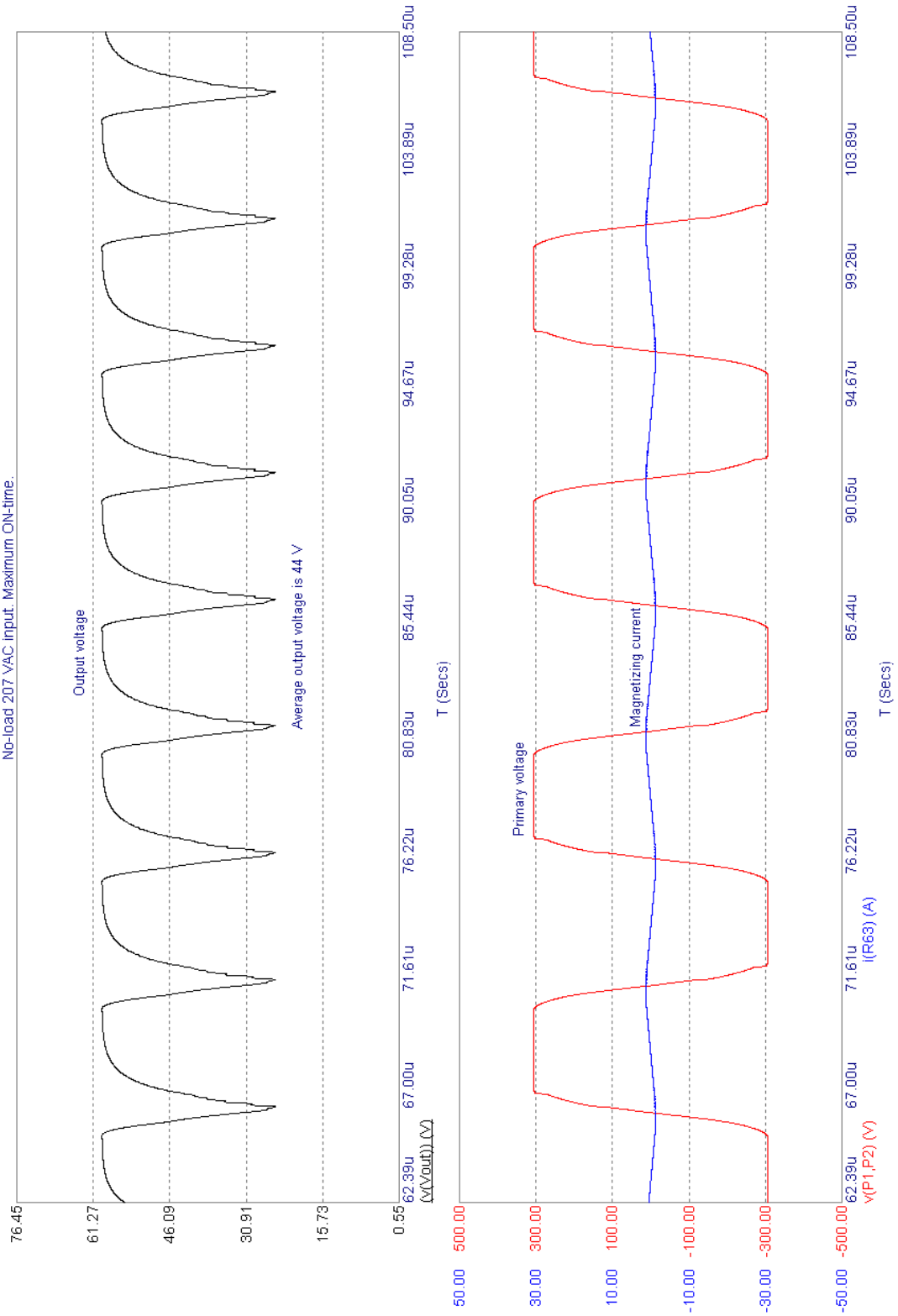

Figure 6
No load w/ 207 VAC input

FOURTH DESIGN CONSTRAINT

According to the fourth design criteria, the converter must be able to supply 150 ADC into a 23.5 VDC welding load (arc) at a 30% duty cycle using ten-minute periods without the steady-state temperatures of the applicable insulations exceeding their respective temperature ratings. From a power capability standpoint, we already know that the converter is capable of meeting this criterion because it is a lower power level requirement than that of the first design requirement, which is 180 ADC at 23 VDC. The challenge in meeting this design requirement is in meeting the thermal requirements. At this output level, the temperatures of the insulation materials must be kept within their applicable ratings. The process used in meeting this criterion is to analyze the power dissipation in the relevant components, and then design the thermal system around that. Those relevant components are the primary and secondary windings of the main transformer, the primary and secondary windings of the isolated gate drive transformers, and the power components mounted on the printed circuit board material. The power components mounted to the printed circuit board consist of the primary switches. The other power components, including the input rectifier diodes and the output rectifier diodes are self-contained modules external to the power converter circuit board which must simply be kept within their electrical device ratings in order to remain within their relevant temperature ratings.

Plots of the output current and voltage is shown on the upper third of Figure 7. This is plotted to verify the power converter is operating at the rated output level of 150 ADC at 23.5 VDC. The instantaneous primary winding current along with its RMS value is plotted in the middle third of Figure 7. Knowledge of the RMS value is needed in order to calculate the power dissipation in the primary windings. Average power dissipation of the four primary switches is shown in the bottom third of Figure 7.

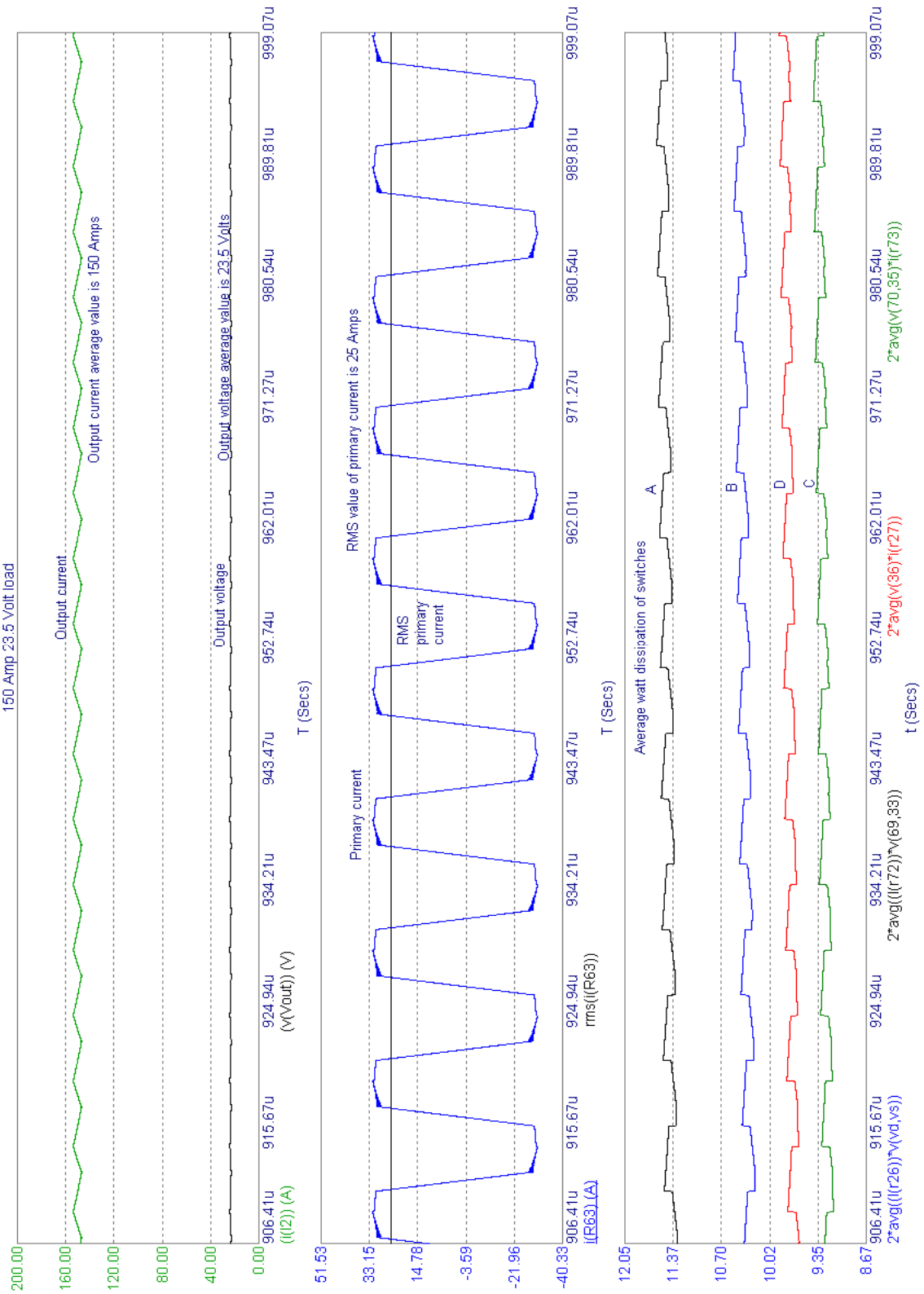

Figure 7
150 Amp 23.5 Volt Load

One might infer that diagonal pairs of switches would have the same amount of power dissipation as each other because they simultaneously conduct the same amount of current during the power transfer stage of the bridge, and hence have the same amount of conduction losses. This is not true however because they each have different amounts of conduction losses during their respective free-wheeling intervals. Note that the power switches do not each experience the same amount of power dissipation in steady-state. The left-leg switches, A and B, both have higher power dissipation than the right-leg switches, C and D. This phenomenon can be explained by first understanding the fact that the right-leg switches lead the left-leg switches with regards to the order of switching operation. In other words, the power transfer stage of the bridge begins when either left-leg switch is turned on since its complementary diagonally-paired switch in the right leg has already been turned on during the preceding free-wheeling interval. As illustrated in Figure 8, since the right-leg switches always lead the left-leg switches, the right-leg switches conduct through their intrinsic body diodes in the reverse direction during their free-wheeling periods while the left-leg switches conduct from drain to source in the forward direction during their free-wheeling periods. This is evident by examining the "I_{ds}" (green) plots of the four switches in Figure 8, and will be explained in more detail in the paragraphs that follow.

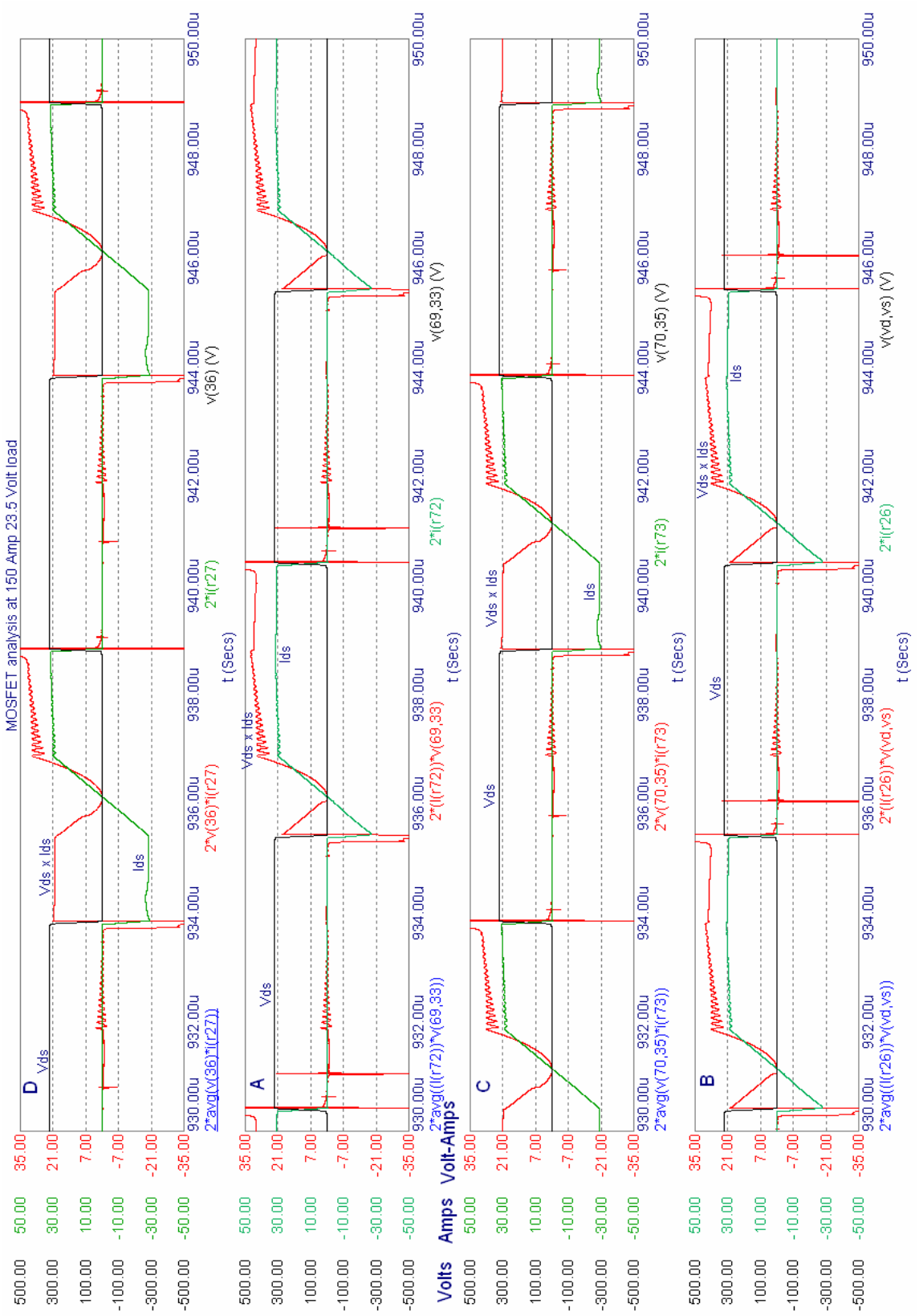

Figure 8

Instantaneous states of the four switches

Since anti-parallel diodes are placed externally across each switch in order to shunt reverse conduction current away from the intrinsic body diode of the MOSFET, the conduction losses in the body diode of the FET are lower than the on-state forward conduction losses in the same FET. As a result, the left-leg switches have higher overall conduction losses than the right-leg switches because they free-wheel in the forward direction while the right-leg switches free-wheel in the reverse direction.

Figure 8 depicts the MOSFET current (green), the drain-source voltage (black), and the instantaneous *apparent* power dissipated (red) for all four switches. The instantaneous apparent power dissipated is not entirely real power dissipated because some reactive power does get transferred across the output capacitance of each MOSFET during switching operations. However, this reactive power "dissipation" averages to zero because the capacitance charges and discharges the same amount of energy. Therefore, the instantaneous apparent power is 100% real power dissipation during conduction and not entirely real power during switching. The plots in Figure 8 correspond to switches D, A, C, B from top to bottom, respectively. D and A form a diagonal pair, with the gate sequence of D leading A (right-leg leading left-leg). C and B form the other diagonal pair, with the gate sequence of C leading B for the same reason. Inspection of Figure 8 supports the fact that the left-leg switches, A and B, free-wheel with forward-conducting current, and hence higher conduction losses, while the right-leg switches, C and D, free-wheel with reverse-conducting current through their intrinsic body diodes.

For instance, immediately following the t = 934.00 μs instant of time in Figure 8, the bridge begins free-wheeling through switches D and B. Inspection of their plots shows forward-conducting current in switch B and reverse-conducting current in switch D. This explains why the average power dissipation of the switches (shown in Figure 7) are not identical.

FIFTH DESIGN CONSTRAINT

The fifth design criteria states that the peak-to-peak ripple in the output current shall not exceed 10%, or 3 Amps, at a 30 Amp average output level. The 200 kHz ripple is caused by the frequency doubling effect of the output rectifier, which converts a 100 kHz AC waveform into a 200 kHz DC output. The component which controls output current ripple is the output inductor. Experimentation in simulation resulted in an inductance value of 21 μH at the 30A/ 15.5V load point. This value was arrived upon by allowing for a 25% margin of safety in the output current ripple, which is 2.4 Amps with a 21 μH output inductor. The inductor is designed to saturate at approximately 80 Amps, so that it does not impede the rise rate of the output current when the welding arc goes into a short-circuit. As was discussed when designing to meet the second design criteria, the converter must be able to supply 400 Amps into a 1 Volt shorted-arc load. The longer time it takes to reach that high current output level, the less probable it is that the arc will re-ignite, depending on other factors affecting the heat transfer and absolute temperature of the weld pool. For this reason, we design the inductor to saturate once the output current ripple becomes unnoticeable due to the higher average

output levels. Plots of the output current ripple and the voltage across the output inductor at a 30A/ 15.5V load point are shown in Figure 9. The upper plot shows the peak-to-peak ripple in the output current is 2.399 Amps. The upper plot also shows the slope of the output current, which is -500 kA/s during demagnetization of the output inductor, and is 1500 kA/s during magnetization of the output inductor. These values, in conjunction with the voltage values across the inductor (lower plot), verify that the 21 μH inductor is properly smoothing the output current ripple by either dropping or sourcing voltage during either demagnetization or magnetization of the choke, without saturation of its core.

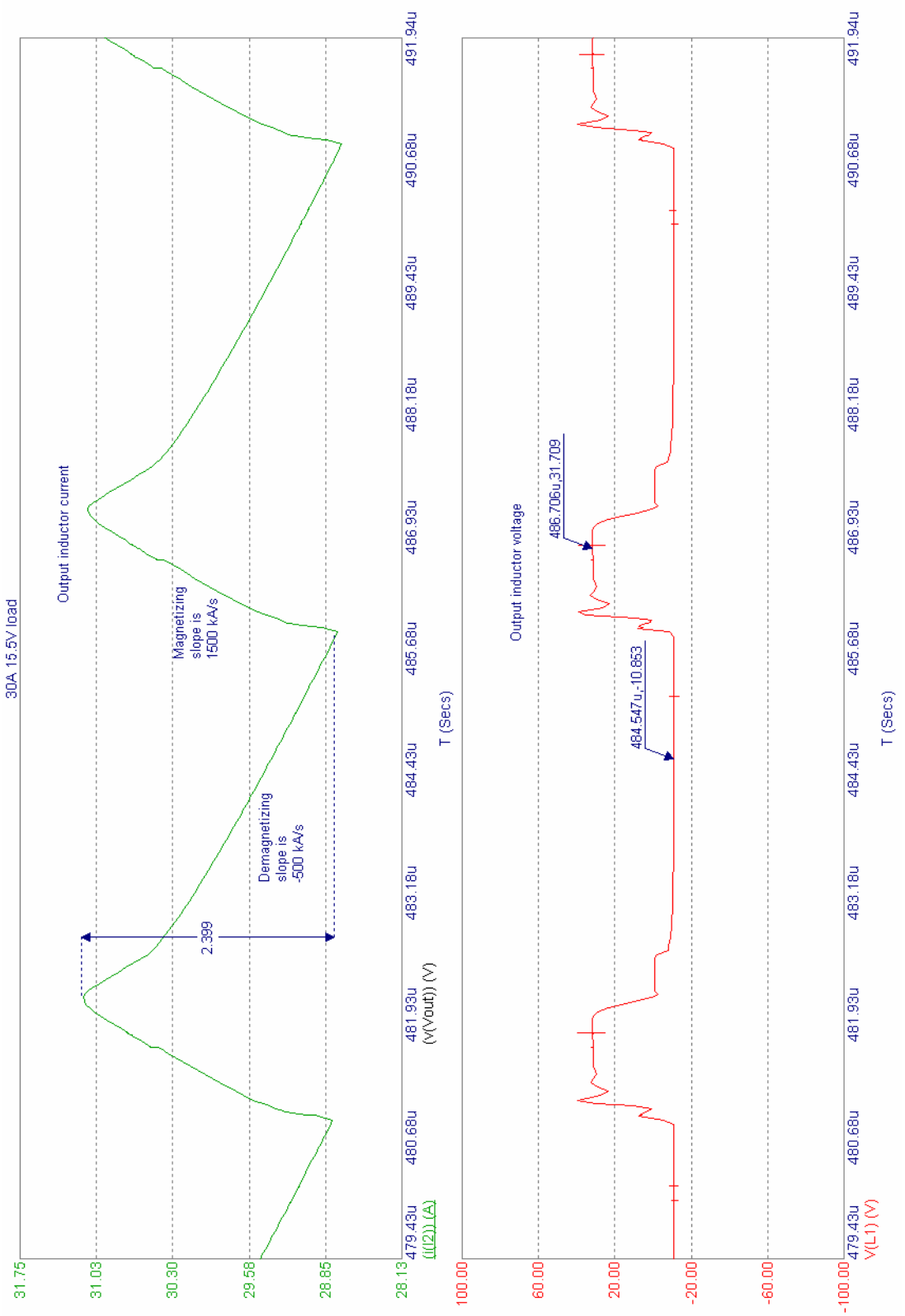

Figure 9

Output current ripple at 30A/ 15.5V load

SIXTH DESIGN CONSTRAINT

In order to meet the sixth design criteria, consideration must be given to both the losses of the system as well as to the thermal design. The thermal design process incorporates primarily a trial and error approach. However, the values attained from Figure 7 give good starting points for the trials. The trial and error approach consists of choosing the primary and secondary conductors' size and geometries, along with choice of heat sink components for the primary switches, building a prototype, running the prototype at the rated output level at a 30% duty cycle using ten-minute periods, recording the winding temperatures and primary switch case temperatures once the prototype reaches steady-state operating temperatures, and then adjusting the design based on the results of the temperature measurements. The choice in the initial design parameter values will primarily impact the development time (number of design iterations) until a final design is reached.

The information gathered from the simulation results of Figure 7, in conjunction with previous design experience are used to determine the "starting points" for the design.

From Figure 7, the switch with the most overall losses is the "A" switch, which dissipates approximately 11.4 Watts. This knowledge of the MOSFET heat dissipation will be used for specifying some heatsink prototypes for the switches.

As for the transformer primary winding, the RMS magnitude of the AC current is 25 Amps. The insulation for isolating the primary and secondary windings is

rated for 155˚C. Assuming a worst-case ambient air temperature of 40˚C, the maximum allowable temperature rise of the windings above ambient temperature during the 150 Amp/ 23.5 Volt/ 30% duty cycle operating condition is 115˚C. This knowledge of the primary current will be used in specifying a transformer prototype.

Since the transformer design utilizes a center-tapped secondary winding, there are 2 halves of the secondary winding that alternately conduct. One half conducts for the positive voltage application on the primary winding; the other conducts for the negative voltage application. In effect, for the 3-minute duration of power delivery from the power converter out of a 10-minute period, each half of the secondary winding is only conducting for a total of 1.5 minutes each. The two halves do, however, share in heat transfer since they are acting as one thermal mass in steady-state. A plot of current through one of the halves of the center-tapped secondary winding is shown in blue in Figure 10. The plot also depicts its RMS value (red) as it approaches a steady-state. The steady-state RMS value is 95 Amps. The total output current is also shown in red. This knowledge of the secondary winding current will also be used in specifying a transformer prototype.

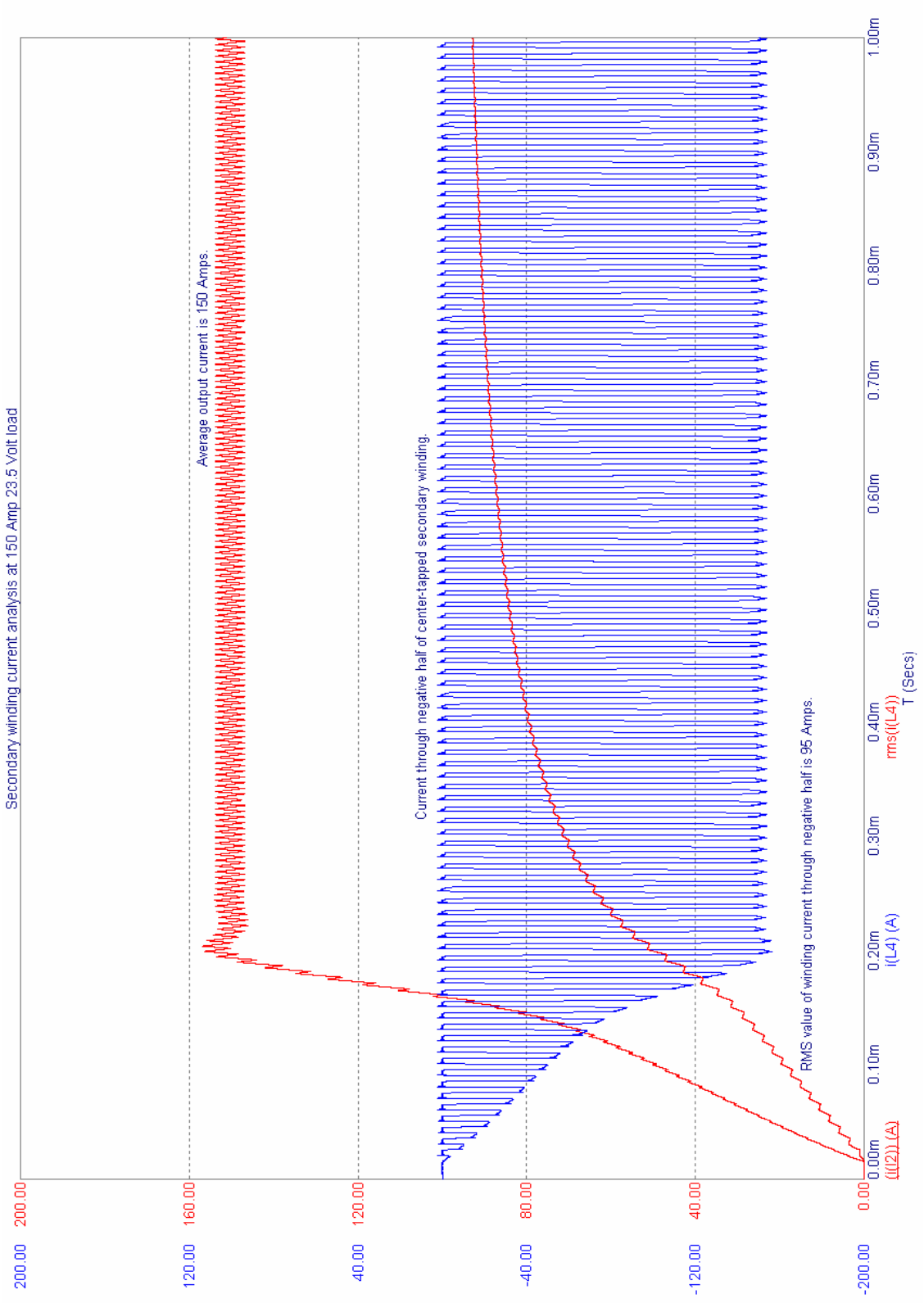

Figure 10

Secondary winding current at 150 Amp 23.5 Volt Load

The windings of the isolated gate drive transformers should also be sized in consideration of the RMS current flowing through their windings under the same output conditions as in the fourth design criteria. Once again by investigation through simulation, the RMS value of the AC current driven through both the primary and secondary windings of the gate drive transformers is approximately 0.5 Amps. The choice of gate drive voltage is ±15 Volts. The maximum gate-source threshold voltage of the driven MOSFET is 4.0 Volts per [12]. Therefore, the applied turn-on gate voltage is almost four times the required gate threshold voltage, which will ensure fast and stable switching. The reasoning for choosing a bipolar gate drive is to ensure fast turn-off times, since switching losses do still exist during turn-off. Negatively biasing the gate during turn-off will reduce switching time and hence losses. This knowledge of the isolated gate drive transformer winding current and voltage will be used for specifying a prototype.

SEVENTH DESIGN CONSTRAINT

Finally, the seventh design criteria states that low cost should be favored over high performance. This was considered in development of the model and will be discussed further in Chapter VI.

CHAPTER VI

ECONOMIC ANALYSIS

The design target cost for the power converter is equivalent to 100% of the cost of the line-commutated transformer-rectifier (LCTR), which the inverter-driven DC-DC converter (IDDD) must compete with in the retail market. This cost is exclusively that required to produce the power converter section of the welder. In the LCTR welder topology, its power converter section consists of the welding arc controls and associated power supplies, the welding transformer, the output rectifier, and the output smoothing filter. In the IDDD welder topology, the power converter section consists of the input rectifier, input storage capacitor, welding arc controls and associated power supplies, the welding transformer, the switching components and any associated snubber circuitry, the output rectifier, and the output smoothing filter. Due to the IDDD's higher operating frequency, the cost advantages of the IDDD topology must be realized in the welding transformer and output smoothing filter, while trying to minimize the added costs of the input rectifier, input storage capacitor, and switching components.

For the purposes of protecting confidential information, actual dollar values of the converter components can not be disclosed. Instead, costs will be represented in terms of “points”, where one point is equal to 1% of the target value. The actual dollar value of the target cost is not disclosed either, however as stated earlier, it is equivalent to 100% of the total cost of LCTR power converter. In other words, the target cost is equal to 100 points. In effect, this point system normalizes the costs based on the existing cost of LCTR.

A breakdown of the power converter costs is shown in Table 1. A Pareto analysis [13] of the costs is shown in Figure 11. The line graph in Figure 11 shows a running total from left to right of the cost of the converter sections as a percentage of the power converter total cost. Percentage values are shown on the right-hand axis. The bar graph in Figure 11 shows the individual costs of each converter section in descending order from left to right. Point values are shown on the left-hand axis.

Converter Section	**Points**
Total	**130.77**
Switches	24.62
Main transformer	23.08
Controls	14.62
Blank (2-layers, Surface-mount)	12.31
Input storage capacitor	11.54
Output rectifier	9.23
Input rectifier	7.69
Gate driver circuits	7.31
Power supplies	7.30
PWM	4.62
Choke	3.85
Feedback	2.31
DSP power supply	1.92
Error amplifier	0.38

Table 1

Cost Estimate of Power Converter (in points)

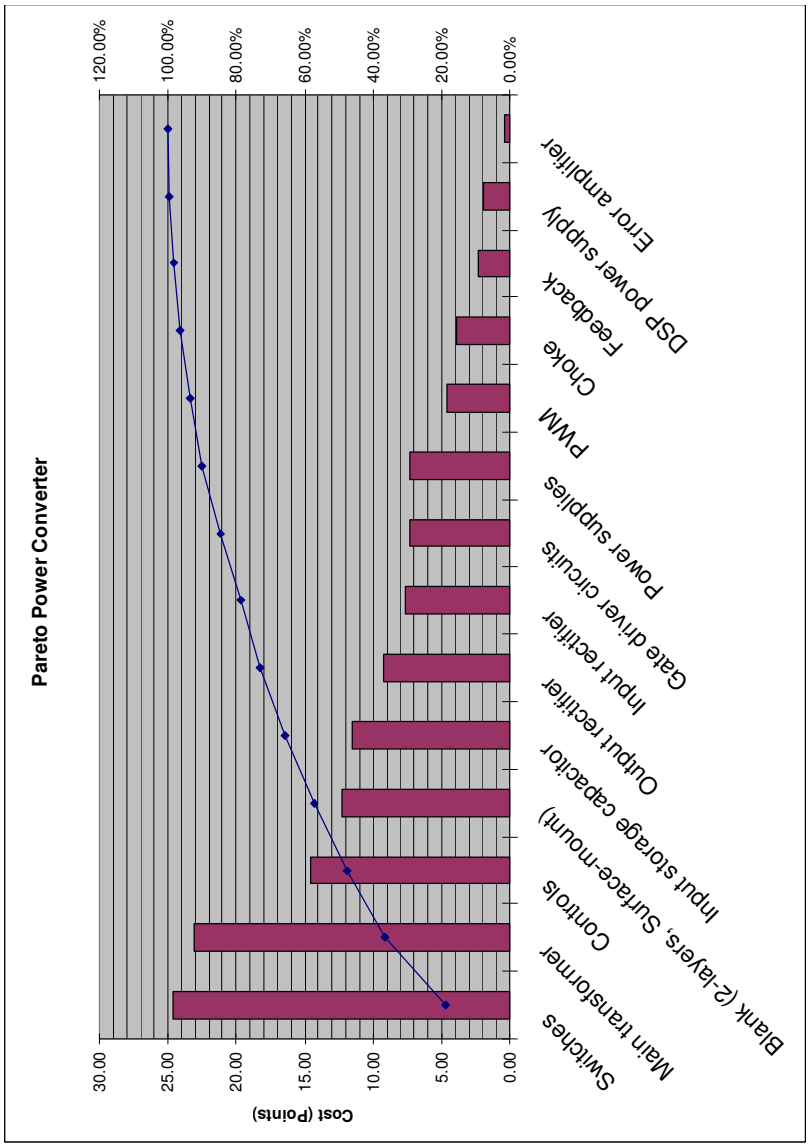

Figure 11
Pareto Analysis of Power Converter Costs (in points)

As one can see from Table 1, the total estimated cost of the power converter is 130.77 points. This cost is 30.77%, over the target for the design. However, given more research in component options and more engineering time, there are some viable options for further reducing the cost.

The most expensive section of the power converter is the switches. These parts were chosen with relative safety margin with regards to their drain current ratings. They are rated for 48 Amps continuous drain current at a case temperature of 100˚C. However, as indicated in Figure 7, the continuous RMS current running through the switches is 25 Amps at the welder's rated output level. There is the potential for saving some cost by using less expensive devices with less silicon, at the expense of perhaps investing in an improved heat sink design. The savings would likely be no better than 1.15 points per device, resulting in a net savings of 4.60 points.

The majority of the cost in the controls section is due to the DSP. The DSP alone costs 10.77 points. The reason it was chosen for this application was because the software development had already been invested into it on a previous design, which was more complex and had more functionality. A less expensive DSP could be chosen for this design at the expense of investing additional software development time. If this strategy were chosen, an additional 6.15 points could be saved from the design.

The power supply section was also borrowed from a previous design, which was not cost-optimal. With some investment in additional engineering time, an additional 2.30 points may potentially be saved from the design.

Given the previously stated options were all pursued, a net cost reduction of 13.05 points could potentially be realized. At which point the total estimated cost of the power converter would be 117.72 points, or 17.72% over the target.

Slightly higher cost does not imply, however, that the IDDD product would not be feasible for the retail market. The IDDD does still have added functionality above and beyond the LCTR. Namely, the IDDD is significantly lighter in weight than the LCTR due to the smaller magnetic devices used. Smaller and lighter is always an important selling feature in the retail market. Secondly, the IDDD is a newer technology than the LCTR. Newer technologies and products are also a strong selling feature in the retail market. Thirdly, the IDDD welding controls are more advanced than those of the LCTR. The welding arc waveform can be more tightly and easily controlled using the DSP controls of the IDDD technology, whereas the LCTR will simply not be able to compete due to its relatively slow line-commutated controls timing. In other words, the IDDD can potentially change its output levels in a matter of tens of microseconds while the LCTR can only change its output levels in a matter of tens of milliseconds, which is three orders of magnitude slower than the IDDD.

The aforementioned three reasons do justify the additional 17.72% of estimated cost over the LCTR product.

CHAPTER VII

CONCLUSION

The goal of this study was to design and analyze an IDDD welding converter that is cost-competitive with LCTR. The final economic analysis yielded an estimated cost that is 30.77% more expensive than the cost of LCTR, and if given the realization of potential cost savings measures, yields a projected cost that is 17.72% more expensive than LCTR. It is not obvious that this can be considered cost-competitive with LCTR. It can be stated however on a non-technical level that its additional features of lighter weight, newer technology, and more advanced welding control options justify the additional 17.72% of cost.

A DC-DC converter for application in a retail welding power source was designed and verified in simulation. Energy efficiency was improved over other conventional converter topologies by using a phase-shifted switching scheme. As a result, a low-cost thermal design can be realized by sinking the small amount of heat losses through the FR4 blank material instead of expensive heat sinks.

Another realized benefit of the phase-shifted switching scheme is lowered EMI. Due to lower EMI in comparison to hard-switched schemes, the PCB blank material may be constructed of only 2 layers instead of needing 4 layers to reduce noise coupling between layers. This presented another facet of cost reduction by design.

A design was successfully specified given the seven design criteria. The choices in component values and ratings were shown to be adequate in meeting the design criteria, while not being excessive or wasteful in cost. Choice in input capacitance, bridge topology, switching components, transformer turns ratio, transformer series inductance, and output inductor were all specified to work in harmony and meet the design criteria given.

Engineering time has been kept minimal by using a previously developed control scheme. A commonly overlooked skill in the engineering discipline is resource management. In this case, there is no need to "re-invent the wheel" when its practical application has already been proven and can easily be scaled to this application. This is an example of wise use of resources.

In presenting this study, a picture of the state of the art in welding power converters is captured in the light of its more cost-competitive technological counterpart. This study educates the engineering audience of what challenges we still face in bringing IDDD technology into the retail market. It also educates the audience of the economical weight of the various power converter components as

the technology stands today. The greatest opportunity exists still today in lowering the cost of switching components. There also exists opportunity for lower cost transformer designs. Achievements in either of these component costs can be the key to launching IDDD welder technology into the retail market, as they alone compromise nearly 40% of the overall power converter cost.

RECOMMENDATIONS FOR FUTURE WORK

Recommendation for future work is to first build and test a prototype. Upon evaluation of the test results, specifically the temperatures of the switching components and transformer materials, these components may potentially be re-sized for a more economical design. A more thorough investigation of the available options in power semiconductor devices should be performed in order to minimize the cost of the switching components.

Another strategy which may have potential for reducing the cost of the switching components is trading silicon for thermal design. In this design, medium-to-high cost semiconductors were chosen in order to favor low cost thermal design. There may exist some cost-optimal solutions, however, that combine medium-to-low cost semiconductors with low-to-medium cost heat sinks, while they have similar functionality as the design chosen in this study. In other words, it may be less expensive to allow higher losses while improving the heat transfer out of the devices, but that needs to be investigated.

REFERENCES

[1] A. Garrigos, J.M. Blanes, J.A. Carrasco, J.L. Lizan, R. Beneito, J.A. Molina. *5 kW DC/DC converter for hydrogen generation from photovoltaic sources*. International Journal of Hydrogen Energy, vol. 35 (2010) pp. 6123-6130.

[2] R. Priewasser, M. Agostinelli, S. Marsili, D. Straeussnigg, M. Huemer OVE. *Comparitive study of linear and non-linear integrated control schemes applied to a Buck converter for mobile applications.* Elektrotechnick & Informationstechnik (2010) 127/4 pp. 103-108.

[3] H. Sugimura, S. Chandhaket, S. Mun, S. Kwon, T. Doi, M. Nakaoka. *Three-Level Phase Shift ZVS-PWM DC-DC Converter with Neutral Point Clamping Diodes and Flying Capacitor for Gas Metal Arc Welding*. Twenty-fifth annual Applied Power Electronics Conference and Exposition, IEEE 2010. pp. 1230-1237.

[4] T. Etoh, H. Manabe, T. Doi, K. Yamaguchi, K. Morimoto, M. Nakaoka. *Novel Input DC Buslines Side Active Soft Switching Cells-Assisted Symmetrical PWM DC-DC Converters with Center-Tapped HF Transformer Link Rectifier*. Twelfth International Conference on Electrical Machines and Systems, 2009. Tokyo, Japan.

[5] C. Wang, Z. Wang, Q. Xu. *Study on Dynamic Characteristics of Inverter Arc Welding Power Supply Based on Double-Loop Control*. Sixth International Power Electronics and Motion Control Conference, 2009. IEEE.

[6] C. Wang, Z. Wang, K. Wang. *Improvements in Designing the Main Circuit of Arc Welding Inverter and the Experimental Verification*. Sixth International Power Electronics and Motion Control Conference, 2009. IEEE.

[7] D. Sha, X. Liao. *Digital Control of Double-Pulsed Gas Metal Arc Welding Machine*. Sixth International Power Electronics and Motion Control Conference (IPEMC) 2009. IEEE.

[8] K. Rauma, O. Laakkonen, J. Luukko, I. Pajari, O. Pyrhonen. *Digital Control of Switch-Mode Welding Machine using FPGA*. 37th IEEE Power Electronics Specialists Conference (PESC) 2006. IEEE.

[9] J. Schupp, W. Fischer, H. Mecke. *Welding arc control with power electronics*. 8th International Conference on Power Electronics and Variable Speed Drives 2000.

[10] Dr. Ray Ridley. *The Nine Most Useful Power Topologies.* Power Systems Design Europe. Oct 2007.

[11] Bill Andreycak. *Phase Shifted, Zero Voltage Transition Design Consideration and the UC3875 PWM Controller*. Unitrode Application Note U-136A. May 1997**.** Texas Instruments, Inc.

[12] Fairchild Semiconductor. *FCH76N60N Datasheet.* May 2010. www.fairchildsemi.com

[13] Nancy R. Tague. *The Quality Toolbox, Second Edition*. ASQ Quality Press, 2004, pp. 376-378.